# Electronic structure of gold: An angle-resolved photoemission study along the Λ line

R. Courths
*Fachrichtung 11.2 (Experimentalphysik), Fachbereich 11 (Physik), Universität des Saarlandes, D-6600 Saarbrücken, Germany*

H. -G. Zimmer and A. Goldmann
*Laboratorium für Festkörperphysik, Universität Duisburg, D-4100 Duisburg, Germany*

H. Saalfeld
*Fachbereich Physik, Universität Osnabrück, D-4500 Osnabrück, Germany*

(Received 13 February 1986)

High-resolution normal-photoemission spectra were recorded for Au(111) with use of synchrotron radiation with photons in the energy range 9 eV $\leq h\nu \leq$ 27 eV. Exploiting direct-transition intensity resonances on $h\nu$ and using results from other measurements, we were able to determine reliable final-state bands along the $\Gamma\Lambda L$ direction up to 18 eV above the Fermi energy and to derive the dispersion of the corresponding occupied $d$ bands. Independent of energy, the experimental final-state bands deviate by about +0.7 eV from a recent density-functional-theory calculation performed by Eckardt, Fritsche, and Noffke [J. Phys. F **14**, 97 (1984)]. The experimental valence bands deviate by about −0.30 eV from theory. Measured critical-point energies (in eV; band indices in parentheses) are $E(\Gamma_8^+(2,3))=-6.01\pm0.02$, $E(\Gamma_7^+(4))=-4.68\pm0.05$, $E(\Gamma_8^+(5,6))=-3.71\pm0.02$, $E(\Gamma_7^-(7))=16.0\pm0.1$, $E(L_{4,5}^+(2))=-6.2\pm0.1$, $E(L_6^+(3))=-5.0\pm0.1$, $E(L_6^+(4))=-3.1\pm0.1$, and $E(L_{4,5}^+(5))=-2.3\pm0.2$.

## I. INTRODUCTION

The one-electron energy-band structure of a solid is essential for an understanding of its electronic properties. The experimental method for mapping band dispersions $E(\mathbf{k})$ of occupied valence states, where $E$ is the energy and $\mathbf{k}$ is the reduced electron momentum, is angle-resolved ultraviolet photoelectron spectroscopy (ARUPS) with vacuum-ultraviolet (vuv) exciting radiation. Provided that the final states for observed direct transitions are known, $E(\mathbf{k})$ may be easily derived (for $\mathbf{k}$ perpendicular to the surface) from normal-emission data with the use of synchrotron radiation. Among the noble metals, the valence bands and several conduction-band points of Cu and Ag have been studied in detail by a number of ARUPS experiments.[1–4] Excellent agreement was found for the occupied valence bands. Some remaining questions concern the final states in photoemission, e.g., the existence of gap states (Refs. 1–4, the references therein) and the dependence of the hole and electron lifetimes on $\mathbf{k}$ and $E$.

In contrast to Cu and Ag, the results of ARUPS experiments on Au (Refs. 5–17) have been the subject of some controversial discussion, mostly concerning the final-state band structure. Some results[8–10] indicate that the experimental $E(\mathbf{k})$ points for the unoccupied bands deviate considerably (up to +4 eV) from the standard-potential calculation of Christensen and Seraphin[18,19] and from the recent density-functional-theory calculation of Eckardt, Fritsche and Noffke.[20] Other investigations[11–14] claim the experimental points above $E_F$ to be in much better agreement with theory (deviations $\lesssim +1$ eV). All groups, however, report that the occupied bands agree much better with the calculations: In general, the experimental points are observed at binding energies larger than predicted. The deviations are rather small for the high-lying $d$ bands at point $X$ [$\simeq -0.1$ eV (Refs. 17 and 21)] and increase to $\simeq -0.3$ eV near the $\Gamma$ point[5,6,14] and along the Λ line.[15,16] Valence-band mapping using synchrotron radiation has been performed by Mills *et al.*[15] and Baalmann *et al.*[16] Both groups assume a free-electron-like final state $E_f=\hbar^2k_\perp^2/2m^*+V_0$. Rather different values for the parameters $m^*$ (electron effective mass) and $V_0$ (inner potential) have been used, however: $m^*=1.17m_0$, $V_0=-3.2$ eV in Ref. 14, and $m^*=m_0$, $V_0=-9.1$ eV in Ref. 15, respectively, where $m_0$ is the free-electron rest mass. Thus there are considerable discrepancies concerning the final-state band structure of Au. We have tried to resolve the controversy by performing new experiments which investigate the empty bands in more detail.

The method used here to determine energy bands is not based on the free-electron final-state approximation.[15,16] It consists of two steps: First, information about special points of final bands along $\Gamma\Lambda L$ is derived, in particular from the dependence of direct-transition intensities on photon energy, and also from secondary-electron features. Second, calculated[20] final-state bands are slightly adjusted to the experimental data. The resulting semiempirical conduction band is then used to obtain the electron momentum perpendicular to the surface, $k_\perp$, and to map the valence-band $E(k_\perp)$ structure along Λ.

## II. EXPERIMENTAL

The experiment was performed at the Berlin Synchrotron Radiation Source [Berlinger Elektronenspeicherring-

 

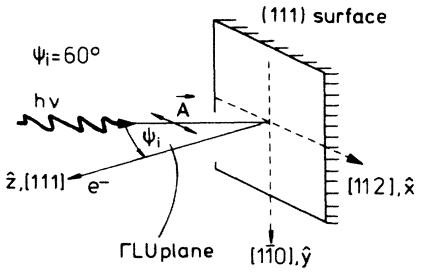


FIG. 1. Experimental geometry employed in the experiments. The light was incident and polarized in the (1$\bar{1}$0) mirror plane of the Au(111) crystal and the photoelectrons were collected along the surface normal.

Gesellschaft für Synchrotronstrahlung m.b.H. (BESSY)] on the toroidal grating monochromator beamline TGM3.[27] Protons with energies $9 \leq h\nu \leq 27$ eV were used. The commercial electron spectrometer (ADES 400, Vacuum Generators Ltd.) is equipped with low-energy electron diffraction (LEED) and retarding-field Auger electron analysis and has been described in detail elsewhere.[28] The total energy resolution (photons plus electrons) was about 100 meV for $9 \leq h\nu \leq 24$ eV and increased to about 150 meV at $h\nu = 27$ eV (full width at half maximum values). The electron angular resolution was $\Delta\theta = 1.5°$ (full angle acceptance). The light was incident in the (1$\bar{1}$0) mirror plane at an angle $\psi_i$ with respect to the surface normal of the crystal (see Fig. 1). The vector potential **A** of the linearly polarized light ($\simeq$90% degree of polarization) was oriented in the plane of incidence ($p$ polarization). At electron-beam currents of about 200 mA in the storage ring, spectra at $h\nu = 20$ eV typically required 3 min to collect about $2 \times 10^4$ counts in the intensity maxima for a 0.02-eV-wide energy channel.

The Au(111) sample, which has already been used for laboratory ARUPS experiments,[29] was cleaned in the UHV chamber by cycles of argon-ion bombardment ($E = 500$ eV) and annealing to approximately 500 °C for several minutes. LEED and the presence and sharpness of the Au(111) surface state in ARUPS[30,31,14] were used to verify that the surface was clean and well ordered.

LEED was also used to orient the (1$\bar{1}$0) mirror plane as plane of incidence. Looking for the intensity maximum and energy minimum of the $sp$ surface state at point $\bar{\Gamma}$,[30,31,14] the orientation of the surface normal was found correct to within $\pm 1°$.

## III. RESULTS

Normal-emission spectra taken with $h\nu = 9$–27 eV in steps of 1 eV are shown in Fig. 2. The direct-transition structures are identified by their dispersion with photon energy and are labeled by the band indices of the initial (occupied) bands 2–6. One also recognizes strong intensity variations with photon energy. Since these intensity resonances will serve for the determination of final-state points, Figs. 3 and 4 show normal-emission spectra at

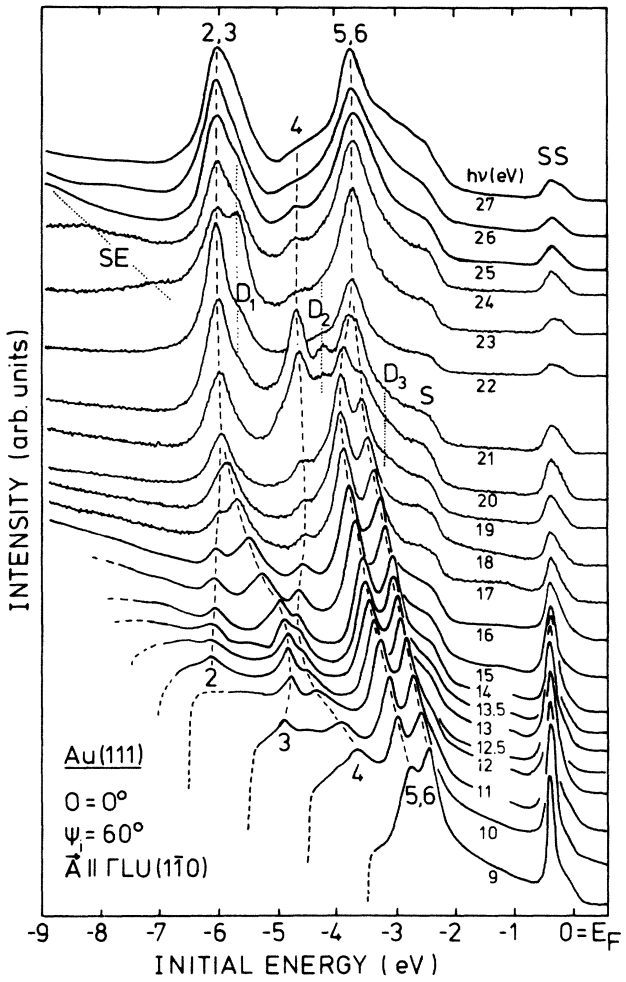


FIG. 2. Normal-emission electron energy distribution curves from Au(111) in the photon energy range $9 \leq h\nu \leq 27$ eV. The curves have been normalized to the maximum count rate. The dispersion of the direct-transition structures, which are labeled by the initial-state band indices, is indicated by the dashed lines. SS is a surface state, $S$ and $D_1$, $D_2$, and $D_3$ are dispersionless structures, SE is a secondary-electron emission feature.

smaller photon-energy steps and the derived dependence of the peak intensities on photon energy, respectively. From data like those shown in Figs. 2 and 3 we determined the initial-state energies $E_i$ of the direct transitions and their dependence on $h\nu$. The results are summarized in Fig. 5.

The peak heights of the direct transition structures (Figs. 2 and 3) are taken as a measure of their intensities. This is justified because no dependence of the linewidth on photon energy is visible. The peak heights were determined assuming a linear background (indicated by a dashed line in the 18.3-eV spectrum) and they are normalized to the secondary-electron intensity at an energy of 8 eV below $E_F$. This normalization led to a smooth decrease of the surface peak intensity (structure SS; see below) with photon energy and (above $h\nu = 17.0$ eV) a constant strength of the shoulder $S$. No line-profile

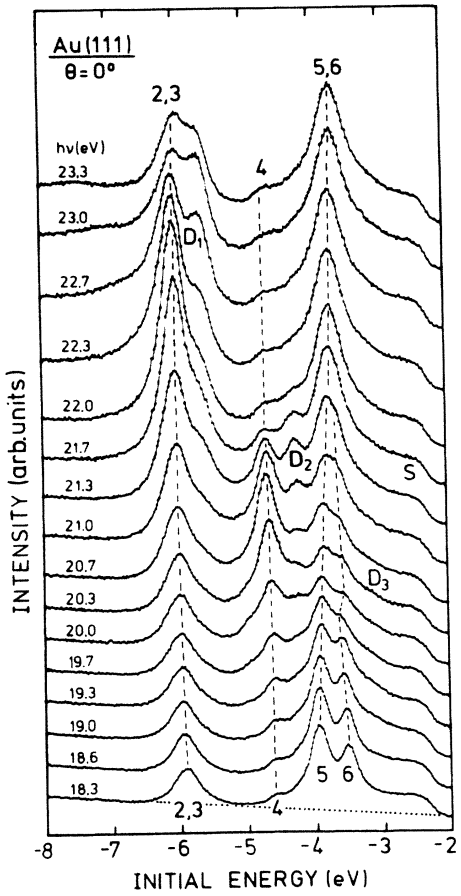


FIG. 3. Normal-emission results from Au(111) with a finer photon-energy mesh. The spectra have been normalized to the same background intensity at 8 eV binding energy. The assumed linear background is indicated for the lowest curve (dotted line).

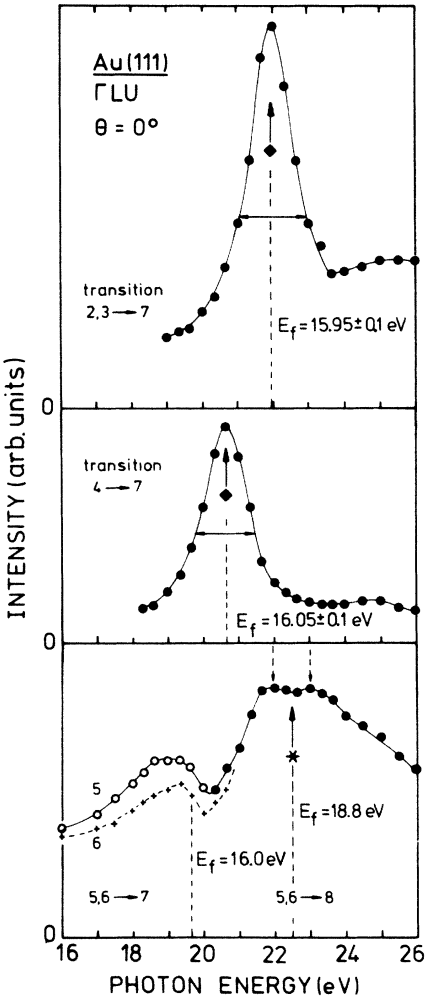


FIG. 4. Peak height of the structures (5,6), 4, and (2,3) in the data of Fig. 3 plotted versus photon energy.

analysis was performed. We note that the photon energies at which resonances occur do not depend on the details of the intensity determination. This was also checked by constant-initial-state spectroscopy for the structures 2, 3, and 4, which show little or no dispersion in the resonance region.

The structure SS at 0.40 eV below the Fermi energy $E_F$ is the well-known *sp*-surface state connected with the $L_6^- - L_6^+$ gap (between the bands 6 and 7) in the center of the surface Brillouin zone at $\bar{\Gamma}$.[30,31,14,16] The intensity of this surface peak is high at low-photon energies and decreases with increasing photon energy, in agreement with the investigation of Baalmann *et al.*[16] A completely analogous behavior of the corresponding surface state at $\bar{\Gamma}$ on Cu(111) had been reported earlier by Knapp *et al.*[32] and Louie *et al.*[33] The apparent asymmetric line shape observed at higher photon energies is due to our finite angular resolution $\Delta\theta$, which in turn leads to increasing momentum spread $\Delta k_{\parallel} \sim \Delta\theta (E_{\rm kin})^{1/2}$: the parabolic dispersion[14] of SS towards $E_F$ results in asymmetric broadening with increasing $E_{\rm kin}$.

Other apparent features in Figs. 2 and 3 are as follows: (i) The shoulder *S* at initial-state energy $E_S \simeq -2.45$ eV, which is visible in the whole series of spectra; (ii) the structures $D_1$, $D_2$, and $D_3$, which are clearly resolved in limited photon-energy ranges at initial-state energies $E_1 = -5.65$ eV, $E_2 = -4.22$ eV, and $E_3 = -3.15$ eV, respectively. Features (i) and (ii) show no dispersion with $h\nu$ and are indicated by the hatched areas in Fig. 5; and (iii) a structure SE with constant final-state energy of $E_f \simeq +15.7$ eV measured with respect to $E_F$. This peak appears in the spectra taken at $h\nu \simeq 23$ eV (Fig. 2) at an "initial" energy $E_{\rm SE} \simeq -7$ eV.

The structure SE is due to secondary-electron emission (SEE). Such Se peaks have also been observed and interpreted in similar studies on Pd(111),[34] Au(111),[15] Pt(111),[15] and Ag(111).[35] Their use for a characterization of final states has been already recognized earlier in the above-mentioned references (which include extensive references to earlier work) and in a recent study of SEE from Cu(001)$c(2\times2)$-Cl.[36] A more detailed study of the SEE from Au(111) will be published elsewhere.[37]

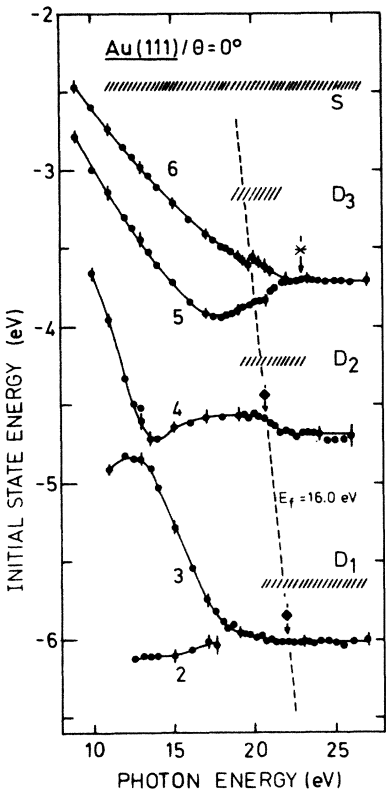


FIG. 5. Energy dispersion with photon energy of the direct-transition structures 2—6 in the normal-emission spectra shown in Figs. 2 and 3. The lines through the data points are guides for the eye. The vertical arrows indicate the resonance energies (see also Fig. 4). Also indicated are the dispersionless structures $S$ and $D_1$, $D_2$, and $D_3$. The dashed line represents a constant final-state energy of 16 eV lowered by the photon energy.

## IV. DISCUSSION

In angle-resolved ultraviolet photoelectron spectroscopy (ARUPS) only $\mathbf{k}_{\parallel}$ is conserved during electron emission through the surface. The vector $\mathbf{k}_{\parallel}$ is completely determined by the kinematical parameters of the experiment. Additional information is therefore required to find $k_{\perp}$. Various methods for the determination of $k_{\perp}$ have been proposed and applied to the noble metals and to some transition metals. Here we only mention the "triangulation method,"[3,8,9,14] the "appearance/disappearance (of direct transitions) methods,"[3] the "surface and gap emission methods,"[3,21] the "Fermi-surface transition method,"[10] and the "zero-slope method."[17,38] They have been described in detail recently[1,2,17] and need not be repeated here. The results obtained with these methods show that the final bands do not disperse like nearly-free electron parabolas, especially not near symmetry points or zone boundaries of the bulk Brillouin zone, where gaps between bands open.[17,38] Often, however, the final bands show a nearly-free electron dispersion along symmetry lines between zone boundaries (e.g., along the $\Lambda$ direction). Band mapping can then be performed in limited $E_f$ and $k_{\perp}$ intervals with rather high accuracy if the parameters $m^*$ and $V_0$ are chosen to fit the "true" final-state band as well as possible.

The experimental band structure of Au along the $\Lambda$ line has been subject to some discussion. Heimann *et al.*[8] and Neddermeyer[9] have applied the triangulation method to Au(112) and Au(111) in order to locate direct transitions along $\Gamma\Lambda L$. They report that the experimental final-state points $E_f(k_\Lambda)$ deviate considerably from Christensen and Seraphin's calculated band 7, by up to $+4$ eV at $E_f \simeq 13$ eV above $E_F$. Christensen[11–13] has argued that the triangulation method (which uses an energy coincidence criterion) does not work in that case; For the photon energy ($h\nu = 16.9$ eV) used by Heimann *et al.*[8] the energy dispersion of the occupied bands is very small, resulting in large experimental errors. This argument was substantiated by Courths *et al.*,[14] who applied the triangulation method to Au(110) and Au(111). The latter authors, however, find that triangulation can be used at $h\nu = 21.2$ eV. They obtain experimental points $E_f(\mathbf{k})$ along $\Lambda$ in fair agreement with Christensen and Seraphin's band structure, with deviations $\lesssim +1$ eV at $E_f \simeq +17$ eV. Courths *et al.*[14] have further shown that despite the failure of the energy coincidence criterion at $h\nu = 16.9$ eV, $E(\mathbf{k})$ information along $\Lambda$ can be derived, if relative peak intensities are compared. Their analysis[14] shows that also at $E_f \simeq 13$ eV

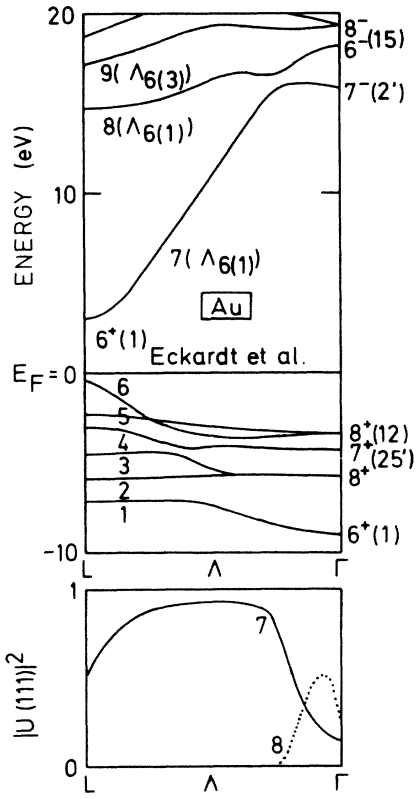


FIG. 6. Top panel: Theoretical band structure for Au along the $\Gamma\Lambda L$ line (Ref. 20). Lower panel: Dependence of the transmission factors $|U(1,1,1)|^2$ on reduced wave vector $k$ along $\Lambda$ for band 7 and band 8, respectively. These curves have not been calculated. They only give the qualitative dependence on $k_\Lambda$ using the quantitative results for Ag (Ref. 3) as a guide.

the experimental band 7 deviates to $\leq +1$ eV from the calculation,[11] in clear disagreement with Refs. 8 and 9. On the other hand, again, Rosei *et al.*[10] found larger deviations, comparable to those reported earlier,[8,9] in other **k** space regions away from $\Lambda$. Their analysis is based on the Fermi-transition method. There was thus a clear motivation for us to reinvestigate the final states of Au in the energy range $E_f \leq 20$ eV.

From the convergence of the direct transitions 2-6 to three lines at $h\nu \simeq 23$ eV (Figs. 2,3, and 5) one can deduce that one samples the region around the $\Gamma$ point. Neglecting possible relaxation shifts (as will be done throughout the following) the corresponding spectra immediately yield the *d*-band energies at $\Gamma$, see Table I. To determine the valence-band dispersion along $\Lambda$ from the data of Fig. 5, the final-state dispersion has to be known. We obtain the energies of the final bands 7 and 8 (see Figs. 6 or 8 for labeling) near $\Gamma$ from the observed intensity resonances (Fig. 4). Such resonances have been quantitatively interpreted, e.g., by Wern *et al.*[3] in a very comparable ARUPS study on Ag(111). Therefore only the main aspects of the interpretation will be given here.

The resonances result from a combined effect of the direct-transition matrix element $\Pi_{fi}$ and a surface-transmission coefficient $t_f$: Within the three-step model of ARUPS (Refs. 42 and 43) the observed emission intensity of a direct transition $i \rightarrow f$ may be written as

$$I_{fi}(k_\Lambda) = |\Pi_{fi}(k_\Lambda)|^2 t_f(k) . \tag{1}$$

In this equation, where

$$\Pi_{fi} = \langle f | \Pi | i \rangle \tag{2a}$$

and

$$\Pi = \mathbf{p} + (h^2/4mc^2)\cdot(\sigma \times \nabla V) , \tag{2b}$$

**p** is the electron momentum operator and $\sigma$ means the electron-spin operator. Both factors appearing in Eq. (1) show strong variations along $\Lambda$ and their combination leads to the intensity resonances as observed in Fig. 4. These effects are explained in some detail in Figs. 6 and 7. Figure 6 shows (upper panel) the band structure of Au along $\Lambda$ as calculated by Eckardt *et al.*[20] The symmetry labels have the following meaning: 7 ($\Lambda_{6(1)}$) indicates that band 7 has $\Lambda_6$ symmetry if the relativistic double-group notation is used (i.e., if spin-orbit coupling is taken into account), while in the nonrelativistic single-group notation the symmetry label is $\Lambda_1$. Similarly, the spin-orbit interaction splits the former $\Lambda_3$ bands into $\Lambda_{6(3)}$ and $\Lambda_{4+5(3)}$, respectively. Only final states of the former $\Lambda_1$ type have group velocities along the surface normal, and therefore only the corresponding bands 7 ($\Lambda_{6(1)}$) and 8 ($\Lambda_{6(1)}$) can couple[42,43] to free-electron states in the vacuum, with **k** normal to the surface. If the bulk final bands are written as Bloch waves,

$$\psi_f(k) = \sum_{\mathbf{G}} U(\mathbf{G}) \exp(i[\mathbf{k}+\mathbf{G}]\cdot\mathbf{r}) , \tag{3}$$

the surface transmission factor is given[42,43] by

$$t_f(k_\Lambda) = |U(1,1,1)|^2 , \tag{4}$$

i.e., the squared amplitude of the plane wave corresponding to the reciprocal lattice vector $\mathbf{G}=(1,1,1)$. The dependence of $|U(1,1,1)|^2$ for bands 7 and 8 is indicated qualitatively in the lower panel of Fig. 6. Note that no calculations of $|U(1,1,1)|^2$ for Au were available. We have therefore adopted the results calculated for Ag along $\Lambda$ (Refs. 3 and 41) and scaled them to Au. Both methods have very similar band structures and this justifies our procedure. We mention that only the qualitative behavior of $|U(1,1,1)|^2$ along $\Lambda$ enters our interpretation of the intensity resonances (Fig. 4).

Similarly, no matrix elements have been calculated yet for Au. However, quantitative results have been presented earlier by Smith and Benbow for Cu (Refs. 39 and 40) and

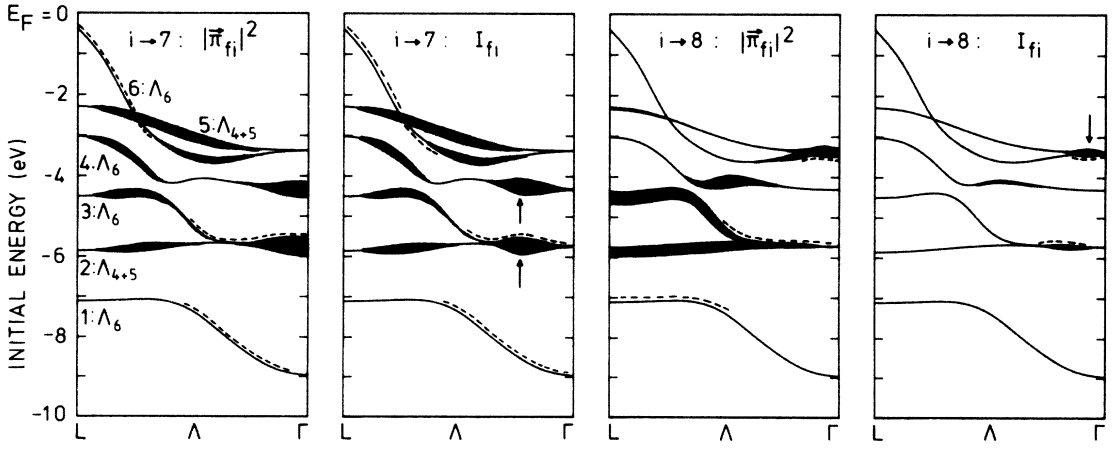


FIG. 7. Dependence along $\Gamma\Lambda L$ of the squared transition matrix elements $|\Pi_{fi}|^2$ and of the photoemission intensities $I_{fi}$ for direct transitions from the occupied bands $i=(1,2,\ldots,6)$ to the band 7 (left panels) and to the band 8 (right panels); light polarized perpendicular to the [111] direction of Au(111). The magnitude of transition strengths and intensities is indicated by the "energy-width" of the valence bands. The dashed lines mark those parts of the bands which are visible with **A**||[111], see also Fig. 1. The data only give the qualitative dependence using the quantitative results for Ag (Refs. 3, 39–41) as a guide.

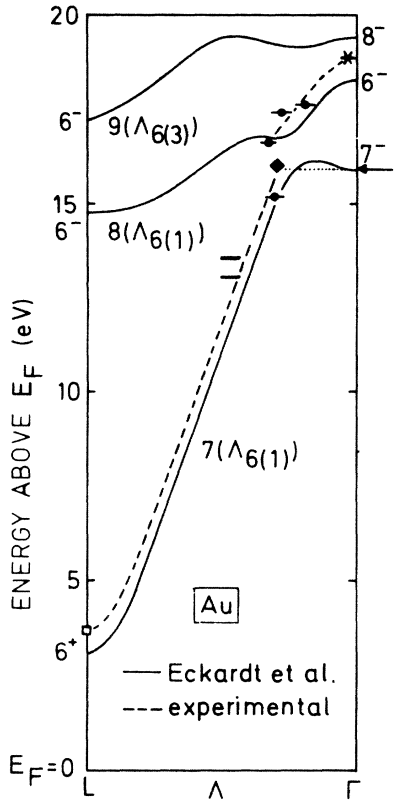


FIG. 8. Band structure of Au along $\Gamma\Lambda L$ above the Fermi energy. The solid lines represent the first principle bands of Eckardt *et al.* (Ref. 20). Results from our analysis of intensity resonances: ◇, ✱. The other experimental $E(k)$ points have been obtained using the triangulation method of ARUPS [—●— and ——, Courths *et al.* (Ref. 14)]; different other techniques (□, see Table I for details); low-energy electron reflectance [←, (Ref. 26)]. The dashed line gives the experimental final-state bands consistent with all data points.

Ag.[41] We have rescaled the results for Ag (Ref. 41) to Au and some typical (qualitative) results are summarized in Fig. 7. This figure reproduces the calculated initial-state bands 1 to 6 and the corresponding intensity behavior for transitions to final band 7 (shown in left two panels) and band 8 (shown in right two panels), respectively. For example, the "energy width" of bands 2 and 3 as plotted in the leftmost panel of Fig. 7 indicates that the transition strength $|\Pi_{fi}|^2$ is largest at $\Gamma$, if the incident photons are linearly polarized perpendicular to the surface normal. If the light is polarized parallel to the [111] direction, only band 6, for example, shows a large $|\Pi_{fi}|^2$ at $L$, as indicated by the dashed-curve labels. After taking $t_f=|U(1,1,1)|^2$ into account [compare Eq. (1)], the situation has changed considerably, see e.g., the second panel from the left: Now the emission intensity $I_{fi}$ exhibits clear resonance behavior at about $k_\Lambda=0.25k_{\Gamma L}$. The reason for this is the drastic decrease of the transmission factor at the onset of the flat-band region of band 7, which shifts the maximum emission intensity away from $\Gamma$. The transitions (5,6)→7 show extremal behavior midway between $\Gamma$ and $L$ and drop to zero intensity at $\Gamma$. At slightly higher photon energy the corresponding transitions (5,6)→8 occur and show maximum intensity in the immediate neighborhood of $\Gamma$. Although the transitions (2,3)→8 and 4→8 show a large $|\Pi_{fi}|^2$ away from $\Gamma$, they are suppressed in this $k_\Lambda$ region due to the vanishing transmission of band 8. Near $\Gamma$ the transitions (2,3)→8 should be detectable, whereas 4→8 should remain invisible. With light polarized parallel to the surface normal, it is those parts of the initial bands, marked by dashed lines in Fig. 7, that mainly contribute.

Inspection of the spectra in Figs. 2 and 3 clearly shows that the direct transitions follow this predicted intensity behavior. Referring to the detailed calculations for Ag along $\Lambda$, it is now easy to correlate the extrema in the intensities (2,3)→7 and 4→7 (Fig. 4) with the onset of the flat branch of band 7 near $\Gamma$. From Fig. 4 the corresponding energy is determined to be 16.0±0.10 eV above the Fermi energy, and this data point is included in Fig. 8 by a solid diamond. The existence of a flat band at 16 eV is supported quantitatively by a sharp peak at 15.9 eV in the low-energy-electron reflectance (LEER) spectrum of Au(111) observed by Jaklevic and Davis[26] at normal incidence. Such a LEER structure was also found for Ag(111).[26] In both metals the photoemission resonances agree within the small experimental error with peaks in the LEER spectra, in support of our interpretation. The SEE feature observed for Au(111), see label SE in Fig. 2, also reflects the flattening of band 7 around 16 eV. SE emission can be observed along the [111] surface normal, if the excited electrons on their deexcitation channels populate regions of a high density of states with dominating $\mathbf{G}=(1,1,1)$ band character. The observed broad SEE peak at 15.7±0.5 eV is thus fully consistent with our analysis.

The situation is somewhat more complex for transitions (5,6)→7 and (5,6)→8. Inspection of Fig. 7 reveals that the emission intensity expected from (5,6)→8 will peak near $\Gamma$, see the arrow in the rightmost panel. The corresponding experimental result is shown by the solid circles in the lowest panel of Fig. 4, indicating a broad intensity resonance at $h\nu=22.5$ eV (asterisk). In fact, one is tempted to identify two peaks, at 22 and 23 eV. However, this interpretation would definitely go beyond the accuracy of our intensity determination (compare also the energy distribution curves reproduced in Fig. 2) and we do not like to oversell the method. Therefore the plateaulike feature around $h\nu=22.5$ eV is identified with band 8 near $\Gamma$ at $E_f=18.8\pm0.5$ eV. What concerns the transitions (5,6)→7, no distinct resonance behavior is to be expected from the estimates shown in Fig. 7. Indeed, the data points collected in Fig. 4 (open circles 5→7, crosses 6→7) do not exhibit any dramatic intensity variation. According to Fig. 7 and the arguments presented earlier, we expect that the emission intensity of (5,6)→7 tends to zero around $E_f=16$ eV. Therefore we correlate the minimum observed at about $h\nu=20$ eV in Fig. 4 with this intensity decrease. The apparent weak maximum near $h\nu=19$ eV would then be an artifact produced by the (roughly) constant intensity of (5,6)→7 below $h\nu\approx19$ eV, its decay to zero intensity around 20 eV, and the superposition of (5,6)→7 with the rapidly increasing intensity of (5,6)→8 in the interval $h\nu=16...21$ eV. Because of this information mix we do not derive final-state energies from the

(5,6)→7 results. We mention that analogous photoemission resonances of direct transitions have already been observed in Pd(111) (Ref. 34) and Au(111) (Ref. 15) normal-emission spectra. They were interpreted correctly as being correlated with the onset of the flattening of band 7. But the intensity enhancement was believed to be due to a high density of final states[15] at Γ. The detailed interpretation could not be given since transition-matrix elements and transmission effects were not discussed.

All available experimental data on empty bands along Λ are summarized in Fig. 8. The present work so far has obtained the intensity-resonance energies of transitions to band 7 (solid diamond in Fig. 8) and to band 8 (asterisk). To get the corresponding $k_\Lambda$ value we proceeded as follows: From the results shown in Fig. 5 we first determined the valence-band dispersions $E_i(k_\Lambda)$ using the final states $E_f(k_\Lambda)$ as calculated by Eckardt *et al.*[20] The result is shown in the left panel of Fig. 9. As can be seen from this figure, the splitting of the bands 5 and 6 in the region $0 \le k_\Lambda \le 0.5 k_{\Gamma L}$ is well described by the theory. The transitions 5→7 and 6→7 reach the flattening of band 7 at $h\nu = 20$ eV (cf. Fig. 5), where the experimental splitting is 0.26 eV. Theory predicts that value at $k_\Lambda = 0.30 k_{\Gamma L}$, and we used this $k_\Lambda$ to plot the diamond in Fig. 8. Theory further tells us that the intensity resonance of the (5,6)→8 transition occurs very near to Γ and this locates the corresponding asterisk in Fig. 8. The energy deviations of our results from the calculated bands are about +0.8 and +0.5 eV, respectively, and these values are in agreement also with other experimental data points obtained earlier and/or by different authors: The $L$-point energy of band 7 ($L_6^+$) has been determined by piezoreflectance,[22] electron tunneling,[23] piezooptical response,[24] and bremsstrahlung isochromat spectroscopy.[25] The average value of $E(L_6^+) = 3.55 \pm 0.10$ eV is plotted in Fig. 8 (open square). It occurs 0.54 eV higher in energy than the calculated value.[18–20] Also included in Fig. 8 are (solid circles and horizontal bars) ARUPS results obtained earlier[14] using the triangulation method, and the energy of a low-energy electron-reflectance peak[26] as indicated by the horizontal arrow near $\Gamma_7^-$. Figure 8 clearly shows that all experimental results are in good overall agreement amongst each other, but deviate by 0.7±0.3 eV on the average from the calculated bands. We can therefore plot experimental final-state bands 7 and 8 as given by the dashed curves in Fig. 8. Critical-point energies are summarized in Table I.

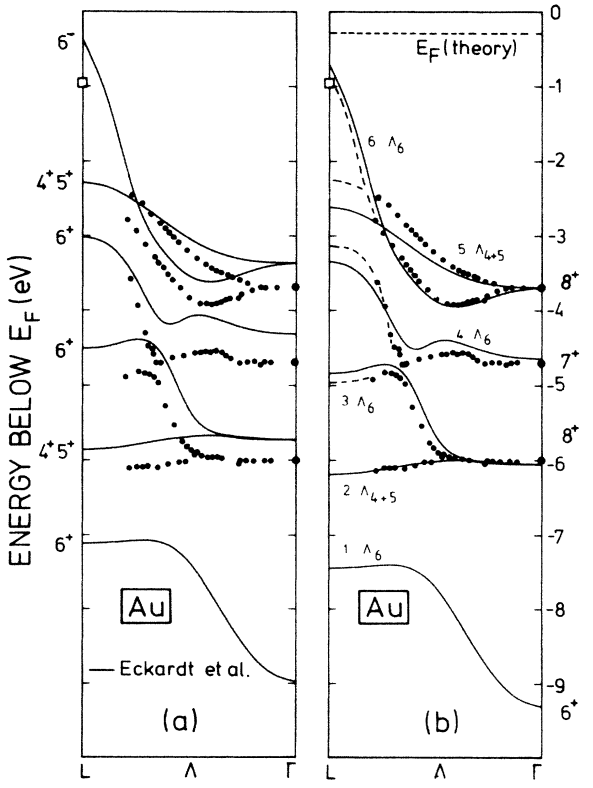


FIG. 9. Band structure of Au below the Fermi energy. The solid lines represent the first-principle bands of Eckhardt *et al.* (Ref. 20). Left: Experimental bands determined using the calculated (Ref. 20) final bands 7 and 8 (Fig. 8). Right: Experimental bands obtained using the experimental final-band structure (Fig. 8). The calculated ground-state bands have been shifted down by 0.30 eV.

The experimental occupied band structure along Λ was then derived using the experimental empty bands. It is shown in the right panel of Fig. 9. To have a better comparison with theory,[20] the latter is shifted downwards in energy by 0.3 eV. A compilation of experimental and theoretical energies at the symmetry points Γ and $L$ is presented in Table I. There is good agreement between our data and those of Baalmann *et al.*,[16] whereas Mills *et al.*[15] found slightly higher values at Γ. We confirm the known result that experiment and theory for the occupied bands differ by 0.3 eV (Ref. 20) to 0.38 eV.[18,19] For the valence bands there is generally a good agreement of the measured dispersion to the calculated one, if a rigid energy shift is taken into account. A slight discrepancy occurs along Λ where band 5 and band 6 cross in theory. The experimental points seem to indicate no crossing. This problem could be clarified by spin-resolved photoemission experiments.[44]

A rigid shift of the theoretical $d$-bands downwards in energy by 0.3 eV to improve the agreement with experiment is not satisfying: For the upper $d$ bands at the $X$ point a shift of only about 0.1 eV would be adequate.[21] Symmetry dependent deviations seem to be effective, as has also been found for Ag.[3] A rigid shift is not compatible with the analysis of optical data, either, as has been discussed by Christensen.[45] Also, the finite temperature in the experiments cannot be responsible for this discrepancy: most of the energy levels move downwards with increasing lattice constant (Ref. 18 and Table I); the theoretical temperature shifts[45] supporting this argument are in agreement with experiment.[46] Therefore we believe that the observed energy difference between the experimental bands and those derived from a ground-state calculation is real. Its quantitative interpretation is a challenge for theory.

The features labeled $S$ and $D_1$ $D_2$, and $D_3$ in Figs. 2, 3, and 5 could not be identified uniquely. A low-energy shoulder like $S$ was also observed for Cu (Ref. 14) and Ag.[35]. Tobin *et al.*[47] ascribed it to the $3z^2 - r^2$ orbital of the outermost atomic layer of Ag(111). Figure 5 suggests

TABLE I. Experimental and theoretical values of valence and conduction bands for gold at the symmetry points $\Gamma$ and $L$. Energies are given in eV relative to the Fermi energy. Errors in parentheses (eV).

| Symmetry label (band index) | Experiment (method) Mills *et al.* (Ref. 15) (ARUPS) | Experiment (method) Baalmann *et al.* (Ref. 16) (ARUPS) | This work (ARUPS) | Theory Eckhardt *et al.* (Ref. 20) | Theory Christensen and Seraphin (Ref. 18) $T=0$ K | Theory Christensen and Seraphin (Ref. 18) dilated lattice | Other work |
|---|---|---|---|---|---|---|---|
| $\Gamma_6^+$ (1) | | | | −9.01 | −9.44 | −9.48 | |
| $\Gamma_8^+$ (2,3) | −5.90 | −6.0 | −6.01(0.02) | −5.75 | −5.65 | −5.91 | |
| $\Gamma_7^+$ (4) | −4.45 | −4.6 | −4.68(0.05) | −4.33 | −4.34 | −4.57 | |
| $\Gamma_8^+$ (5,6) | −3.55 | −3.65 | −3.71(0.02) | −3.38 | −3.29 | −3.61 | |
| $\Gamma_7^-$ (7) | | | 16.0(0.1) | 15.88 | 15.58 | 15.17 | 15.9[a] |
| $\Gamma_6^-$ (8) | | | 18.8(0.5) | 18.29 | 18.03 | 17.35 | |
| $L_6^+$ (1) | | −7.80(0.15)[b] | | −7.14 | −7.35 | −7.45 | |
| $L_{4,5}^+$ (2) | | −6.23(0.15)[b] | −6.20(0.05)[c] | −5.88 | −5.82 | −6.05 | |
| $L_6^+$ (3) | | −4.88(0.1)[b] | −5.00(0.05)[c] | −4.52 | −4.34 | −4.77 | |
| $L_6^+$ (4) | | | −3.2(0.1)[c] | −3.02 | −2.81 | −3.20 | |
| $L_{4,5}^+$ (5) | | | −2.3(0.1)[c] | −2.29 | −2.10 | −2.50 | −2.5[d] |
| $L_6^-$ (6) | | | | −0.37 | −0.72 | −0.97 | −1.0[d]<br>−1.0(±0.1)[e]<br>−1.01(±0.04)[f]<br>−1.1(±0.1)[g] |
| $L_6^+$ (7) | | | | 3.01 | 3.01 | 2.41 | +3.6[d]<br>+3.65(0.05)[e]<br>+3.56(0.02)[f]<br>+3.4(0.1)[g] |

[a]Jaklevic and Davis (low-energy-electron reflectance) (Ref. 26).
[b]Free-electron final-state approximation for $40 \leq h\nu \leq 55$ eV.
[c]Extrapolated using the theoretical dispersions as a guide.
[d]Szczepanek and Glosser (piezoreflectance) (Ref. 22).
[e]Jaklevic and Lambe (electron tunneling, $T$-4.2 K) (Ref. 23).
[f]Chen and Segall (piezooptical response) (Ref. 24).
[g]Marel *et al.* (bremsstrahlung isochromat spectroscopy) (Ref. 25).

that $D_1$, $D_2$, and $D_3$ could be surface resonances, split off the $\Gamma$ points by about half an eV. Experiments are in progress to check this idea.

## V. SUMMARY

We summarize our main results as follows: We have studied normal emission from Au(111) for photon energies between 9 and 27 eV. By a careful analysis of intensity resonances in direct transitions, and by using experimental results obtained with several techniques by other authors, we could determine the experimental final-state bands. These enabled us to derive the energy dispersion $E(k_\perp)$ of occupied bands along most of the $\Gamma\Lambda L$ direction. Several critical-point energies below and above $E_F$ could be determined at $\Gamma$ and $L$, with an accuracy of at least 0.1 eV. Comparison to a recent band-structure calculation by Eckardt *et al.*[20] yields generally good overall agreement. The quantitative agreement is almost perfect, if a rigid shift to the calculated bands is applied of about $+0.7$ eV above $E_F$ and $-0.3$ eV below $E_F$. Several features not due to direct transitions could be clearly identified. No unique interpretation, however, can be offered yet. We conclude that the bulk bands of Au along $\Gamma L$ are experimentally known with a typical accuracy of 0.1 eV, in the energy range from about 6 eV below $E_F$ to about 19 eV above $E_F$.

## ACKNOWLEDGMENTS

This work was performed at the Berlin Synchrotron Radiation Source [Berlin Elektronenspeicherring-Gesellschaft für Synchrotronstrahlung m.b.H. (BESSY)] and we thank the BESSY staff, especially W. Braun, for help. We also thank F. Müller for his skilled experimental assistance. Support for this work was provided by the Deutsche Forschungsgemeinschaft and the Bundesministerium für Forschung und Technologie.

[1]F. J. Himpsel, Adv. Phys. **32**, 1 (1983), and references therein.
[2]R. Courths and S. Hüfner, Phys. Rep. **112**, 53 (1984) and references therein.
[3]H. Wern, R. Courths, G. Leschik, and S. Hüfner, Z. Phys. B **60**, 293 (1985), and references therein.
[4]A. Goldman, H.-G. Zimmer, R. Courths, and H. Saalfeld, Solid State Commun. **57**, 523 (1986).
[5]P. O. Nilsson and L. Ilver, Solid State Commun. **17**, 667 (1975).
[6]P. Heimann and H. Neddermeyer, J. Phys. F **7**, L37 (1977).
[7]G. V. Hansson and S. A. Flodström, Phys. Rev. B **18**, 1572 (1978).
[8]P. Heimann, H. Miosga, and H. Neddermeyer, Solid State Commun. **29**, 463 (1979).
[9]H. Neddermeyer, Solid State Commun. **40**, 809 (1981).
[10]R. Rosei, R. Lässer, N. V. Smith, and R. L. Benbow, Solid State Commun. **35**, 979 (1980).
[11]N. E. Christensen, Solid State Commun. **37**, 57 (1981).
[12]N. E. Christensen, Solid State Commun. **38**, 309 (1981).
[13]N. E. Christensen, Phys. Rev. B **24**, 2263 (1981).
[14]R. Courths, H. Wern, U. Hau, B. Cord, V. Bachelier, and S. Hüfner, J. Phys. F **14**, 1559 (1984); Solid State Commun. **49**, 989 (1984).
[15]K. A. Mills, R. F. Davis, S. D. Kevan, G. Thornton, and D. A. Shirley, Phys. Rev. B **22**, 581 (1980).
[16]A. Baalmann, M. Neumann, H. Neddermeyer, W. Radlik, and W. Braun, Ann. Israel Phys. Soc. **6**, 351 (1983).
[17]M. Wöhlecke, A. Baalmann, and M. Neumann, Solid State Commun. **49**, 217 (1984).
[18]N. E. Christensen and B. O. Seraphin, Phys. Rev. B **4**, 3321 (1971).
[19]N. E. Christensen, Phys. Rev. B **13**, 2698 (1976).
[20]H. Eckardt, L. Fritsche, and J. Noffke, J. Phys. F **14**, 97 (1984).
[21]H. Wern, G. Leschik, U. Hau, and R. Courths, Solid State Commun. **50**, 581 (1984).
[22]P. Szczepanek and R. Glosser, Solid State Commun. **15**, 1425 (1974).
[23]R. C. Jaklevic and J. Lambe, Phys. Rev. B **12**, 4146 (1975).
[24]A. Chen and B. Segall, Solid State Commun. **18**, 149 (1976).
[25]D. v. d. Marel, G. A. Sawatsky, R. Zeller, F. U. Hillebrecht, and J. C. Fuggle, Solid State Commun. **50**, 47 (1984).
[26]R. C. Jaklevic and L. C. Davis, Phys. Rev. B **26**, 5391 (1982).
[27]W. Braun and G. Jäkisch, Ann. Israel Phys. Soc. **6**, 30 (1983).
[28]A. Baalmann, Ph.D. thesis, University of Osnabrück, West Germany, 1984.
[29]U. Hau, diploma work, University of Saarland, Saarbrücken, West Germany, 1985.
[30]P. Heimann, H. Neddermeyer, and H. P. Roloff, J. Phys. C **10**, L17 (1977).
[31]Z. Hussain and N. V. Smith, Phys. Lett. **66A**, 492 (1978).
[32]J. A. Knapp, F. J. Himpsel, and D. E. Eastman, Phys. Rev. B **19**, 4952 (1979).
[33]S. G. Louie, P. Thiry, R. Pinchaux, Y. Pétroff, D. Chandesris, and J. Lecante, Phys. Rev. Lett. **44**, 549 (1980).
[34]F. J. Himpsel and D. E. Eastman, Phys. Rev. B **18**, 5236 (1978).
[35]J. G. Nelson, S. Kim, W. J. Gignac, R. S. Williams, J. G. Tobin, S. W. Robey, and D. A. Shirley, Phys. Rev. B **32**, 3465 (1985).
[36]H.-G. Zimmer, D. Westphal, K. K. Kleinherbers, A. Goldmann, and A. Richard, Surf. Sci. **146**, 425 (1984).
[37]H.-G. Zimmer, A. Goldmann, and R. Courths (unpublished).
[38]A. Baalmann, M. Neumann, W. Braun, and W. Radlik, Solid State Commun. **54**, 583 (1985).
[39]N. V. Smith, Phys. Rev. B **19**, 5019 (1979).
[40]N. V. Smith, Phys. Rev. B **21**, 4331 (1980).
[41]R. L. Benbow and N. V. Smith, Phys. Rev. B **27**, 3144 (1983).
[42]N. V. Smith in *Photoemission in Solids,* edited by M. Cardona and L. Ley (Springer, Berlin, 1978), Vol. 1.
[43]H. Przybylski, A. Baalmann, G. Borstel, and M. Neumann, Phys. Rev. B **27**, 6669 (1983).
[44]A. Eyers, F. Schäfers, G. Schönhense, U. Heinzmann, H. P. Oepen, K. Hünlich, J. Kirschner, G. Borstel, Phys. Rev. Lett. **52**, 1559 (1984).
[45]N. E. Christensen, Phys. Rev. B **20**, 3205 (1979).
[46]P. Heimann and H. Neddermeyer, Solid State Commun. **26**, 279 (1978).
[47]J. G. Tobin, S. W. Robey, L. E. Klebanoff, and D. A. Shirley, Phys. Rev. B **28**, 6169 (1983).